Coupled Systems Mechanics, *Vol. 6, No. 4 (2017) 377-398*
DOI: https://doi.org/10.12989/csm.2017.6.4.377

Inclined cable-systems in suspended bridges for restricting dynamic deformations

Ioannis Raftoyiannis*[1], Theodore Konstantakopoulos[2a] and George Michaltsos[1b]

[1]*National Technical University of Athens, Department of Civil Engineering, 15780, Greece*
[2]*University of Thessaly, Greece*

(Received May 11, 2017, Revised July 11, 2017, Accepted July 12, 2017)

Abstract. The present paper deals with the influence of the inclination of cables' system on the decrease of the lateral-torsional motion because of dynamic loadings. For this goal, a mathematical model is proposed. A 3-D analysis is performed for the solution of the bridge model. The theoretical formulation is based on a continuum approach, which has been widely used in the literature to analyze such bridges. The resulting uncoupled equations of motion are solved using the Laplace Transformation, while the case of the coupled motion is solved through the use of the potential energy. Finally, characteristic examples are presented and useful results are obtained.

Keywords: suspension bridges; footbridges; dynamic behavior; damping systems

1. Introduction

A lot of work has been reported during the last 100 years, dealing with the dynamic response of railway bridges and later of highway bridges, under the influence of moving loads. Extensive references to the literature on this subject can be found in the excellent Frýba's book (1972).

Two early interesting contributions, in this area, exist thanks to Stokes (1849) and Zimmerman (1896). In 1905, Krýlov gave a complete solution to the problem of the dynamic behavior of a prismatic bar acted upon by a load of constant magnitude, moving with a constant velocity. In 1922, Timoshenko solved the same problem, but for a harmonic pulsating moving force. Another pioneer work on this subject was presented in 1934, by Inglis, in which numerous parameters were taken into account. In 1951, Hillerborg gave an analytical solution to the previous problem, by means of Fourier's method.

Despite the availability of high speed computers, most of the methods used today for analyzing bridge vibration problems are essentially based on the Inglis's or Hillerborg's early techniques. Relevant publications are the ones of Saller (1921), Jeffcot (1929), Steuding (1934), Honda *et al.* (1982), Gillespi (1993), Green and Cebon (1994), Green *et al.* (1995), Zibdeh and Reckwitz

∗Corresponding author, Associate Professor, E-mail: rafto@central.ntua.gr
[a]Research Associate, E-mail: theokons@teemail.gr
[b]Professor, E-mail: michalts@central.ntua.gr

http://www.techno-press.org/?journal=csm&subpage=8 ISSN: 2234-2184 (Print), 2234-2192 (Online)

Fig. 1 Nervi's solution with inclined cables

(1996), Lee (1996), Michaltsos *et al.* (1996), Xu and Genin (1997), Foda and Abduljabbar (1998), Michaltsos (2001, 2002), Li *et al.* (2013), Greco *et al.* (2013), Lonetti and Pascuzzo (2014a,b), Raftoyiannis *et al.* (2014), Baloervic *et al.* (2016) and Sun *et al.* (2016).

On the other hand, in practice, in spite of the great number of works, for over 50 years, bridges (as also other constructions which are acted upon by dynamic loads) have been designed to account for dynamic loads, by increasing the design live loads by a semi-empirical "impact factor" or "dynamic load allowance".

Recently, there have been many programs of research, in different countries, on the effect of the characteristics of a bridge, or a vehicle, on the dynamic response of a bridge. We can mention the programs in U.S.A. (1977), in U.K. and Canada (1983), in the Organization for Economic Cooperation and Development (O.E.C.D.) (1992), in Switzerland (1972) etc.

Although there are also important publications in this field, we must especially refer to the important experimental research by Cantieri (1991), on different models of moving loads.

During the last decades, cable bridges (Stay-cable or Suspended bridges) have received great attention and ware used to cover long spans because of their reduced erection cost.

Both types are characterized by their special shape and aesthetic. Long span bridges, based on cable stayed or suspension bridge system, have been used in different frameworks. The use of the cable system types is strictly connected to structural, economic and practical reasons. The combination of the two systems (of suspended and cable-stayed ones) appears able to provide notable advantages in the long span bridges, and to guarantee stable and safe erection processes due to the suspension cable system, while, simultaneously, a reduced deformability of the girder is expected due to the reinforcement effect of the additional stay cables.

A serious problem of the long-span cable bridges is the lateral instability caused by dynamic loadings, as for example earthquake or wind pressure or buffeting forces, Zhang and Yu (2015) and Zhang and Zhang (2016). The usual classical confrontation of the problem is the deck's strengthening, but it is proved as a non-economic one. In some cases, mainly in foot-bridges, there was applied a system of cables that had an inclination to the horizontal, in order to minimize the lateral motion produced by crowd loading.

The Millennium footbridge in London (2000-2002), the Peace footbridge in London Derry (2011), the River Dee footbridge in Breamer (at design stage), the Happy Pontist Scottish Bridge (2009) are some of bridges with inclined systems of cables.

In long span cable stayed bridges we have very often inclined pylons, mainly for aesthetic

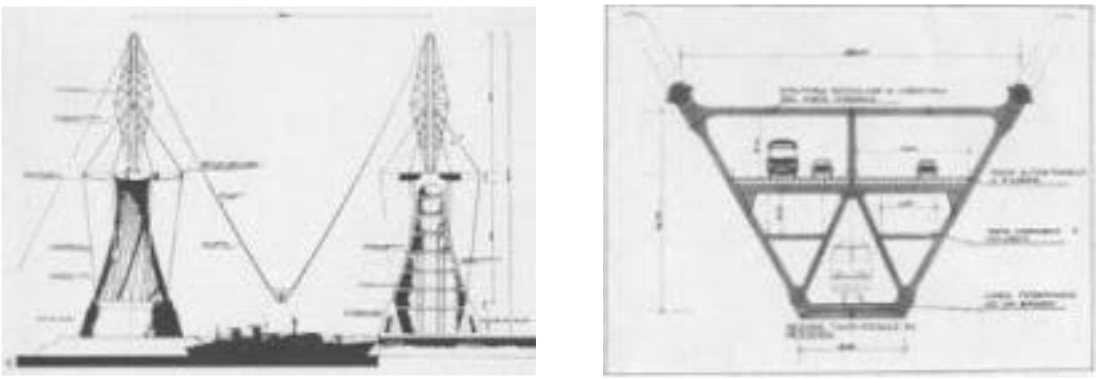

Fig. 2 The bridge's pylons and cross-section

reasons.

Until today there are not erected long-span suspension bridges with inclined cable systems.

At the end of the 1960's, Nervi was amongst engineers asked to propose a design for a bridge across the Messina Straits, between Italy and Sicily. The depth of water in the Straits meant that the bridge had to cross about 3km in a single span (although other designers, such as Leonhardt, were still proposing designs with deep-water piers at the same time-see the book by Richard Scott).

Nervi's contemporary and compatriot Sergio Musmeci proposed a peculiar suspension bridge where the suspension cables are hung not directly from towers, but from cable stays which are in turn suspended from super-towers beyond the ends of the main bridge. Musmeci's idea included lateral cables either side of the deck to provide it with transverse stability.

Although this was an odd design, the proposal by Nervi was even stranger.

Nervi sought to achieve lateral stability by inclining the main suspension cables away from the deck (see Fig. 1), so that the deck hangers are no longer vertical, and the towers supporting the main cables are separated by a considerable distance.

The towers are hyper-paraboloid (see Fig. 2) concrete shells capped with enormous steel assemblies. They're restrained by stays to resist the incredible horizontal forces they would have to carry.

The deck itself appears to be a trapezoidal concrete box (see Fig. 2) which would be incredibly heavy and attract enormous wind loading.

Authors do not find either notable research studies on this field or other communications related to constructional or other objects that set on thinking designers or constructors, except papers dealing with footbridges and using cables in order to minimize its oscillations caused by human crowd like Nakamura and Kawasaki (2006), Eckhard and Ott (2006), Roberts *et al.* (2008), Ingolfsson and Georgakis (2011, 2012) and moving loads like Greco *et al.* (2013) and Lonetti and Pascuzzo (2014b).

The present paper deals with the influence of the inclination of cables' system on the decrease of the lateral-torsional motion because of dynamic loadings. For this goal a mathematical model is proposed for inwards or outwards inclination of the cable system, where the height and inclination of the pylons are thoroughly investigated.

A 3-D analysis is performed for the solution of the bridge model. The theoretical formulation is based on a continuum approach, which has been widely used in the literature to analyze bridges.

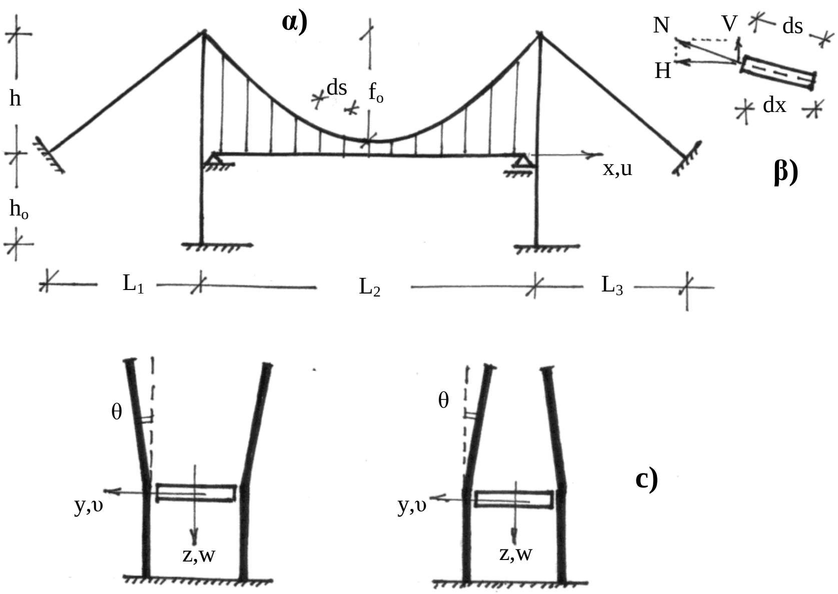

Fig. 3 Schematic of the studied bridge and cable-systems

The resulting uncoupled equations of the motion are solved using the Laplace Transformation, while the case of the coupled motion is solved through the use of the potential energy. Finally, characteristic examples are presented and useful results are obtained.

2. Introductory concepts

a. The bridge and the cable-systems studied are shown in Fig. 3(a). Above the deck level, the pylons are inclined by angle θ which may be clockwise or counterclockwise.

b. Under the action of dead loads it is υ=w=φ=0, while the initial stress of cables is N_o with components H_o and V_o (Fig. 3(b)).

c. They are valid the following relations from the theory of suspension bridges

$$\left.\begin{aligned} & H = H_o + H_e\,, \quad S = -H\cdot(f+\Delta f)''\,, \quad H_e = -\frac{f''}{L_c / E_c F_c}\cdot\int_0^L \Delta f\,dx\,, \\ & f(x) = \frac{4f_o}{L^2}(Lx - x^2), \quad H_o = \frac{S_o L^2}{8f_o}\,, \quad H_o = -\frac{g}{f''} \\ & L_c = \left(1 + \frac{8f_o^2}{L_2^2}\right) + \frac{(L_1^2+h^2)^{3/2}}{L_1^2} + \frac{(L_3^2+h^2)^{3/2}}{L_3^2} \end{aligned}\right\} \tag{1a}$$

where with index “o” are symbolized the tensions and forces caused by dead loads while with index “e” the ones caused by live and dynamic loadings.

d. The above system is analyzed into the systems of Fig. 4, consisting of one vertical with sag f_V, f_{Vo} and stress of the hangers S_V and one horizontal with f_H, f_{Ho} and S_H.

The following relations are valid

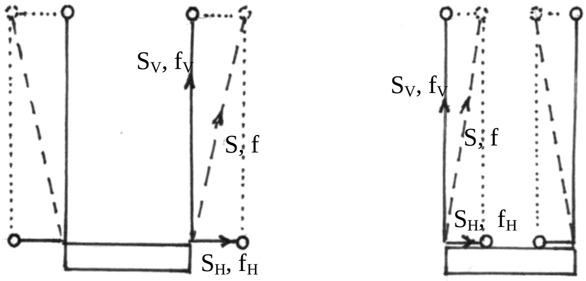

Fig. 4 Analysis of the cable system in two equivalent systems

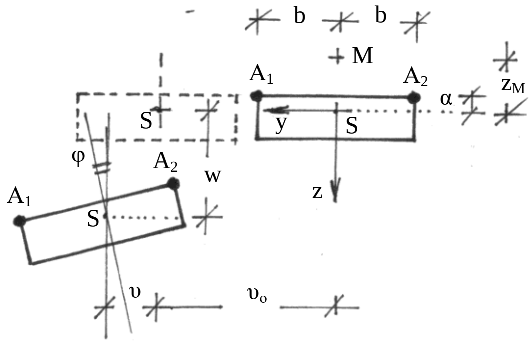

Fig. 5 The displacements of the deck

$$\left.\begin{aligned} S_V &= S\cdot\cos\theta \quad & f_{Vo} &= f_o\cos\theta \\ S_H &= S\cdot\sin\theta \quad & f_{Ho} &= f_o\sin\theta \end{aligned}\right\} \tag{1b}$$

According to the theory of cables, their tensions will be

$$\left.\begin{aligned} H_V &= \frac{S_V L^2}{8f_{Vo}} = \frac{S\cdot\cos\theta\cdot L^2}{8f_o\cos\theta} = \frac{S\cdot L^2}{8\cdot f_o} = H \\ H_H &= \frac{S_H L^2}{8f_{Ho}} = \frac{S\cdot\sin\theta\cdot L^2}{8f_o\sin\theta} = \frac{S\cdot L^2}{8\cdot f_o} = H \end{aligned}\right\} \tag{1c}$$

e. Separating the deck and showing its motion because of the action of a horizontal load, we get Fig. 5, showing the displacement of a cross-section of the deck, where υ_o is the ground motion and $\upsilon, w,$ and φ are the displacements and the angle of rotation of the cross-section's gravity center.

Assuming that the cables are anchored at points A_1 and A_2, the following additional displacements $d\upsilon$ and dw because of φ are valid: $d\upsilon = \alpha\cdot\varphi$ and $dw = b\cdot\varphi$, and therefore the entire displacements of points A_1 and A_2 will be

$$\left.\begin{aligned} &\text{From Fig. 6a:} \quad \left.\begin{aligned} \upsilon_{A1} &= \upsilon + \alpha\varphi \\ w_{A1} &= w + b\varphi \end{aligned}\right\} \quad \left.\begin{aligned} \upsilon_{A2} &= \upsilon - \alpha\varphi \\ w_{A2} &= w - b\varphi \end{aligned}\right\} \\ &\text{From Fig. 6b:} \quad \left.\begin{aligned} \upsilon_{A1} &= \upsilon - \alpha\varphi \\ w_{A1} &= w + b\varphi \end{aligned}\right\} \quad \left.\begin{aligned} \upsilon_{A2} &= \upsilon + \alpha\varphi \\ w_{A2} &= w - b\varphi \end{aligned}\right\} \end{aligned}\right\} \tag{1d}$$

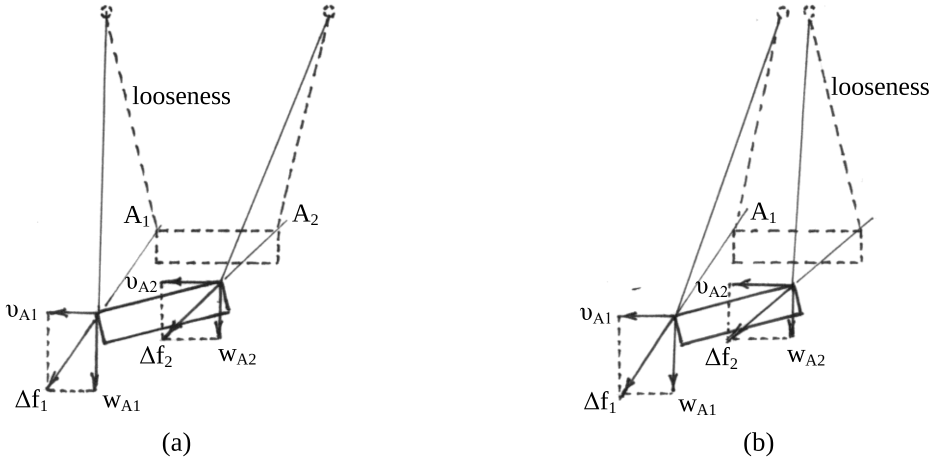

Fig. 6 The displacements of the hangers

3. Analysis

3.1 The acting forces

In Figs. 6(a) and 6(b), one can see the displacements of points A_1 and A_2 (where they are joined the hangers). One can observe that applying the positive signs for υ, w, and φ, some displacements cause additional strain of hangers while others cause looseness of hangers (see Figs. 6(a) and 6(b)). This remark is taken into account in the following analysis. In addition, we remember that: $\Delta f << f$.

For easier understanding the following procedure, we analyze the cable-system in two others (Fig. 4), consisting of one vertical with sag $f_V = f\cos\theta$ and hangers' tensions $S_V = S\cos\theta$, and another horizontal with sag $f_H = f\sin\theta$ and hangers' tensions $S_H = S\sin\theta$.

3.1.1 The vertical forces

Marking by the index "o" the forces without dynamic loadings and by "e" the additional forces because of dynamic loads we have

$$\left.\begin{aligned} P_z &= g + p_z(x,t) - c_z\dot{w} - m\ddot{w} - (S_{V1} + S_{V2}) = \\ &= g + p_z(x,t) - c_z\dot{w} - m\ddot{w} + (H_{V1} + H_{Ve1})(f_V + w_1)'' + (H_{V2} + H_{Ve2})(f_V + w_2)'' = \\ &= g + p_z(x,t) - c_z\dot{w} - m\ddot{w} + 2H_o f_V'' + H_o(w_1'' + w_2'') + H_{Ve1} f_V'' + H_{Ve2} f_V'' \end{aligned}\right\} .$$

or finally

$$\left.\begin{aligned} & P_z = p_z(x,t) - c_z\dot{w} - m\ddot{w} + 2H_o w'' - \frac{2 f_V''^{\,2}}{L_{cV}/E_c F_c} \cdot \int_0^L w\,dx \\ & \text{with :} \\ & f_V'' = -\frac{8 f_o}{L^2} \cdot \cos\theta , \quad \text{and} \quad L_{cV} = L_2 \cdot \left(1 + \frac{8 f_o^2 \cdot \cos^2\theta}{L_2^2} \right) + \frac{(L_1^2 + h_V^2)^{3/2}}{L_1^2} + \frac{(L_3^2 + h_V^2)^{3/2}}{L_3^2} \\ & \text{and:} \quad h_V = h \cdot \cos\theta \end{aligned}\right\} \qquad (2)$$

where Eqs. (1) are taken into account and also that $\Delta f \ll f$.

3.1.2 The horizontal forces

Following a similar procedure with §3.1.1 we have

$$P_y = p_y(x,t) - c_y(\dot{\upsilon}+\dot{\upsilon}_o) - m(\ddot{\upsilon}+\ddot{\upsilon}_o) + S_{H1} - S_{H2} =$$
$$= p_y(x,t) - c_y(\dot{\upsilon}+\dot{\upsilon}_o) - m(\ddot{\upsilon}+\ddot{\upsilon}_o) - (H_{H1} - H_{He1})f_H'' + (H_{H2} + H_{He2})f_H''$$

Because of Eqs. (1) we finally obtain

$$\left.\begin{array}{l} P_y = p_y(x,t) - c_y(\dot{\upsilon}+\dot{\upsilon}_o) - m(\ddot{\upsilon}+\ddot{\upsilon}_o) - \dfrac{2f_H''^2}{L_{cH}/E_cF_c}\cdot\displaystyle\int_0^L \upsilon dx \\ \text{with :} \\ f_H'' = -\dfrac{8f_o}{L^2}\cdot\sin\theta\,, \quad \text{and} \quad L_{cH} = L_2\cdot\left(1+\dfrac{8f_o^2\cdot\sin^2\theta}{L_2^2}\right) + \dfrac{(L_1^2+h_H^2)^{3/2}}{L_1^2} + \dfrac{(L_3^2+h_H^2)^{3/2}}{L_3^2} \\ \text{and:} \quad h_H = h\cdot\sin\theta \end{array}\right\} \quad (3)$$

where $\upsilon_o(t)$ is the soil motion, while it is taken into account that a positive υ_{A1} brings about looseness of the cable 1 (Fig. 6(a)), while a positive υ_{A2} brings about looseness of the cable 2 (Fig. 6(b)).

3.1.3 The torsional moments

Taking into account §3.1.1 and 3.1.2 we obtain

$$M_x = m_x(x,t) - c_\varphi\dot{\varphi} - J_{px}\ddot{\varphi} - S_{V1}b + S_{V2}b - (z_M - \alpha)S_{H1} + (z_M - \alpha)S_{H2}$$

or finally

$$M_x = m_x(x,t) - c_\varphi\dot{\varphi} - J_{px}\ddot{\varphi} - \frac{2b^2\cdot f_V''^2}{L_{cV}/E_cF_c}\int_0^L \varphi dx + \frac{2(z_M-\alpha)f_H''^2}{L_{cH}/E_cF_c}\int_0^L \upsilon dx \quad (4)$$

3.2 The equations of motion

Taking into account Eqs. (2), (3), (4) and that the external loadings can be expressed as relations of t, the complete equations of motion are given by the following expressions

$$\left.\begin{array}{l} EI_y w'''' - 2H_o w'' + c_y\dot{w} + m\ddot{w} = p_z(x,t) - B_V\displaystyle\int_0^L w dx \\ EI_z(\upsilon+\upsilon_o)'''' - EI_z\cdot z_M\varphi'''' + c_z(\dot{\upsilon}+\dot{\upsilon}_o) + m(\ddot{\upsilon}+\ddot{\upsilon}_o) = p_y(x,t) - B_H\displaystyle\int_0^L \upsilon dx \\ EI_\omega\varphi'''' - EI_z\cdot z_M(\upsilon+\upsilon_o)'''' - GI_d\varphi'' + c_\varphi\dot{\varphi} + I_{px}\ddot{\varphi} = m_t(x,t) - b^2\cdot B_V\displaystyle\int_0^L \varphi dx + (z_M-\alpha)B_H\displaystyle\int_0^L \upsilon dx \\ \text{with :} \quad B_V = \dfrac{2f_V''^2}{L_{cV}/E_cF_c}\,, \quad B_H = \dfrac{2f_H''^2}{L_{cH}/E_cF_c} \\ \text{and :} \quad p_y(x,t) = p_y(x)\cdot f_y(t)\,, \quad p_z(x,t) = p_z(x)\cdot f_z(t)\,, \quad m_x(x,t) = m_x(x)\cdot f_x(t) \end{array}\right\} \quad (5)$$

4. Doubly symmetric cross-section

For a bridge which the deck has a cross-section of double symmetry, will be $z_M = 0$, α=0, and therefore Eqs. (5) become

$$\left.\begin{aligned} &EI_y w'''' - 2H_o w'' + c_y \dot{w} + m\ddot{w} = p_z(x,t) - B_V \int_0^L w dx \\ &EI_z \upsilon'''' + c_z \dot{\upsilon} + m\ddot{\upsilon} = p_y(x,t) - c_z \dot{\upsilon}_o - m\ddot{\upsilon}_o - B_H \int_0^L \upsilon dx \\ &EI_\omega \varphi'''' - GI_d \varphi'' + c_\varphi \dot{\varphi} + I_{px} \ddot{\varphi} = m_t(x,t) - b^2 B_V \int_0^L \varphi dx \end{aligned}\right\} \tag{6}$$

In this case we observe that all equations are independent each other and therefore they can be solved separately.

4.1 The vertical motion

In order to solve Eq. (6a), we are searching for a solution of the form

$$w(x,t) = \sum_{\rho=1}^{n} W_\rho(x) \cdot T_\rho(t) \tag{7a}$$

where $T_\rho(t)$ are the time functions under determination and $W_\rho(x)$ are functions arbitrarily chosen that satisfy the boundary conditions. As such functions we choose the shape functions of an one span beam with axial force $2H_o \sin\theta$, given by the following expressions (12)

$$\left.\begin{aligned} &W_\rho(x) = c_1 \left(\sin\lambda_1 x - \frac{\sin\lambda_1 L}{\mathrm{Sinh}\lambda_2 L} \cdot \mathrm{Sinh}\lambda_2 x \right) \\ &\text{where}: \quad \lambda_1 = \sqrt{-\frac{H_o}{EI_y} + \sqrt{\left(\frac{H_o}{EI_y}\right)^2 + \frac{m\omega_{y\rho}^2}{EI_y}}}\,, \quad \lambda_2 = \sqrt{\frac{H_o}{EI_y} + \sqrt{\left(\frac{H_o}{EI_y}\right)^2 + \frac{m\omega_{y\rho}^2}{EI_y}}} \end{aligned}\right\} \tag{7b}$$

while $\omega_{y\rho}$ are given by the relation

$$\left.\omega_{y\rho} = \sqrt{\frac{\rho^4\pi^4 EI_y}{mL^4} + \frac{2\rho^2\pi^2 H_o}{mL^2}} \qquad \rho = 1, 2, 3, \ldots\ldots \right\} \tag{7c}$$

Introducing (7a) into (6a) we obtain

$$EI_y \sum_{\rho=1}^{n} W_\rho'''' T_\rho - 2H_o \sum_{\rho=1}^{n} W_\rho'' T_\rho + c_y \sum_{\rho=1}^{n} W_\rho \dot{T}_\rho + m \sum_{\rho=1}^{n} W_\rho \ddot{T}_\rho = p_z - B_V \int_0^L \sum_{\rho=1}^{n} W_\rho T_\rho dx \tag{8a}$$

Remembering that $W_\rho(x)$ satisfies the equation of free motion

$$EI_y W_\rho'''' - 2H_o W_\rho'' - m\omega_{y\rho}^2 W_\rho = 0 \tag{8b}$$

Eq. (8a) becomes

$$m\sum_{\rho=1}^{n} W_\rho \ddot{T}_\rho + c_y \sum_{\rho=1}^{n} W_\rho \dot{T}_\rho + m\sum_{\rho=1}^{n} \omega_{y\rho}^2 W_\rho T_\rho = p_z - B_V \int_0^L \sum_{\rho=1}^{n} W_\rho T_\rho dx \tag{8c}$$

Multiplying the above by $W_\rho(x)$ and integrating from 0 to L we get

$$\ddot{T}_\rho + \frac{c_y}{m}\dot{T}_\rho + \omega_{y\rho}^2 T_\rho = \frac{\int_0^\alpha p_z W_\rho dx}{m\int_0^L W_\rho^2 dx}\cdot f_z(t) - \frac{\int_0^L W_\rho dx}{m\int_0^L W_\rho^2 dx}\cdot B_V \int_0^L \sum_{\rho=1}^{n} W_\rho T_\rho dx \tag{8d}$$

with α from Fig. 5.

In order to solve the above system of Eqs. (8d), we employ the Laplace Transformation with initial conditions $T_\rho(0) = \dot{T}_\rho(0) = 0.$ Therefore, we set

$$\left.\begin{aligned} &LT_\rho(t) = G_\rho(s) \\ &Lf_z(t) = F_z(s) \\ &L\dot{T}_\rho(t) = s\cdot G_\rho(s) \\ &L\ddot{T}_\rho(t) = s^2\cdot G_\rho(s) \end{aligned}\right\} \tag{8e}$$

Hence, the system (8d) becomes

$$\left.\begin{aligned} &a_{\rho1}G_1 + a_{\rho2}G_2 + \cdots + a_{\rho k}G_k + \cdots a_{\rho\rho}G_\rho + \cdots a_{\rho n}G_n = B_\rho \\ &\text{where:} \\ &a_{\rho k} = \frac{B_v \int_0^L W_\rho dx \int_0^L W_k dx}{m\int_0^L W_\rho^2 dx}, \quad a_{\rho\rho} = \frac{B_v \left(\int_0^L W_\rho dx\right)^2}{m\int_0^L W_\rho^2 dx} + s^2 + \frac{c_y}{m}\cdot s + \omega_{y\rho}^2 \\ &B_\rho = \frac{\int_0^\alpha p_z W_\rho dx}{m\int_0^L W_\rho^2 dx}\cdot F_z(s) \end{aligned}\right\} \tag{8f}$$

and finally

$$T_\rho(t) = L^{-1}G_\rho(s) \tag{8g}$$

4.2 The lateral motion

In order to solve Eq. (6b), we are searching for a solution of the form

$$\upsilon(x,t) = \sum_{\rho=1}^{n} V_\rho(x)\cdot R_\rho(t) \tag{9a}$$

where $R_\rho(t)$ are the time functions under determination and $V_\rho(x)$ are functions arbitrarily chosen that satisfy the boundary conditions. As such functions we choose the shape functions of an one span beam, given by the following expressions (12)

$$V_\rho(x) = c_1 \cdot \sin\frac{\rho\pi x}{L_2} \quad \Bigg\} \tag{9b}$$

while $\omega_{z\rho}$ are given by the relation

$$\omega_{z\rho} = \sqrt{\frac{\rho^4\pi^4 E I_z}{m L_2^4}} \qquad \rho = 1, 2, 3, ... \quad \Bigg\} \tag{9c}$$

Introducing (9a) into (6b) and following the procedure of §4.1, we conclude to the system

$$\ddot{R}_\rho + \frac{c_z}{m}\cdot\dot{R}_\rho + \omega_{z\rho}^2 R_\rho = \frac{f_y(t)\int_0^L p_y V_\rho dx - (c_z\dot{\upsilon}_o + m\ddot{\upsilon}_o)\int_0^L V_\rho dx}{m\int_0^L V_\rho^2 dx} - \frac{B_H\int_0^L V_\rho dx}{m\int_0^L V_\rho^2 dx}\cdot\int_0^L\sum_{\rho=1}^n V_\rho R_\rho dx \tag{9d}$$

In order to solve the above system (12d) we use the Laplace Transformation with initial conditions: $R(0) = \dot{R}(0) = 0$. We put

$$\left.\begin{array}{l} LR_\rho(t) = K_\rho(s), \quad L\dot{R}_\rho(t) = s\cdot K_\rho(s), \quad L\ddot{R}_\rho(t) = s^2\cdot K_\rho(s) \\ Lf_z(t) = F_z(s), \quad L\upsilon_o(t) = U_o(s), \quad L\dot{\upsilon}_o(t) = s\cdot U_o(s), \quad L\ddot{\upsilon}_o(t) = s^2\cdot U_o(s) \end{array}\right\} \tag{9e}$$

Therefore, the system (12d) becomes

$$\left.\begin{array}{l} b_{\rho1}K_1 + b_{\rho2}K_2 + \cdots + b_{\rho k}K_k + \cdots b_{\rho\rho}K_\rho + \cdots + b_{\rho n}K_n = \Gamma_\rho \\ \text{where:} \\ b_{\rho k} = \dfrac{B_H\int_0^L V_\rho dx\int_0^L V_k dx}{m\int_0^L V_\rho^2 dx}, \quad b_{\rho\rho} = \dfrac{B_H\left(\int_0^L V_\rho dx\right)^2}{m\int_0^L V_\rho^2 dx} + s^2 + \dfrac{c_z}{m}\cdot s + \omega_{z\rho}^2 \\ \Gamma_\rho = \dfrac{\int_0^L p_y V_\rho dx}{m\int_0^L V_\rho^2 dx}\cdot F_z(s) - \dfrac{\int_0^L V_\rho dx}{m\int_0^L V_\rho^2 dx}\cdot(c_z\cdot s + m\cdot s^2)\cdot U_o(s) \end{array}\right\} \tag{9f}$$

and finally

$$R_\rho(t) = L^{-1}K_\rho(s) \tag{9g}$$

4.3 The torsional motion

In order to solve Eq. (6c), we are searching for a solution of the form

$$\varphi(x,t)=\sum_{\rho=1}^{n}\Phi_\rho(x)\cdot Z_\rho(t) \tag{10a}$$

where, $Z_\rho(t)$ are the time functions under determination and $\Phi_\rho(x)$ are functions arbitrarily chosen that satisfy the boundary conditions. As such functions we choose the shape functions in torsion of a single span beam, given by the following equations

$$\left.\begin{aligned}
&\Phi_\rho(x)=c_1\left(\sin k_1 x-\frac{\sin k_1 L}{\operatorname{Sinh} k_2 L}\cdot \operatorname{Sinh} k_2 x\right)\\
&\text{where:}\quad k_1=\sqrt{-\frac{G\,I_d}{2E\,I_w}+\sqrt{\left(\frac{G\,I_d}{2E\,I_w}\right)^2+\frac{I_{px}\omega_{\varphi\rho}^2}{E\,I_w}}}\\
&\qquad\qquad k_2=\sqrt{\frac{G\,I_d}{2E\,I_w}+\sqrt{\left(\frac{G\,I_d}{2E\,I_w}\right)^2+\frac{I_{px}\omega_{\varphi\rho}^2}{E\,I_w}}}
\end{aligned}\right\} \tag{10b}$$

while $\omega_{\varphi\rho}$ are given by following the relation

$$\left.\omega_{\varphi\rho}=\sqrt{\frac{\rho^4\pi^4 E\,I_w}{I_{px}L^4}+\frac{\rho^2\pi^2 G\,I_d}{I_{px}L^2}},\quad \rho=1,2,3,.......\right\} \tag{10c}$$

Introducing (13a) into (9c) and following the procedure of §4.1 we conclude to the system

$$\ddot Z_\rho+\frac{c_\varphi}{m}\dot Z_\rho+\omega_{\varphi\rho}^2 Z_\rho=\frac{\int_0^\alpha m_x\Phi_\rho dx}{I_{px}\int_0^L\Phi_\rho^2 dx}\cdot f_x(t)-\frac{b^2B_V\int_0^L\Phi_\rho dx}{I_{px}\int_0^L\Phi_\rho^2 dx}\cdot\int_0^L\sum_{\rho=1}^{n}\Phi_\rho Z_\rho dx \tag{11a}$$

In order to solve the above system (14a) we use the Laplace Transformation with initial conditions $Z_\rho(0)=\dot Z_\rho(0)=0$. We put

$$\left.\begin{aligned}
&LZ_\rho(t)=N_\rho(s)\,,\quad Lf_x(t)=F_x(s)\\
&L\dot Z_\rho(t)=s\cdot N_\rho(s)\,,\quad L\ddot Z_\rho(t)=s^2\cdot N_\rho(s)
\end{aligned}\right\} \tag{11b}$$

Therefore, the system (14a) becomes

$$\left.\begin{aligned}
&\gamma_{\rho 1}N_1+\gamma_{\rho 2}N_2+\cdots+\gamma_{\rho k}N_k+\cdots+\gamma_{\rho\rho}N_\rho+\cdots+\gamma_{\rho n}N_n=\Delta_\rho\\
&\text{where:}\\
&\gamma_{\rho k}=\frac{b^2B_V\int_0^L\Phi_\rho dx\int_0^L\Phi_k dx}{I_{px}\int_0^L\Phi_\rho^2 dx},\quad \gamma_{\rho\rho}=\frac{b^2B_V\left(\int_0^L\Phi_\rho dx\right)^2}{I_{px}\int_0^L\Phi_\rho^2 dx}+\left(s^2+\frac{c_\varphi}{I_{px}}\cdot s+\omega_{\varphi\rho}^2\right)\\
&\Delta_\rho=\frac{\int_0^\alpha m_x\Phi_\rho dx}{I_{px}\int_0^L\Phi_\rho^2 dx}\cdot F_x(s)
\end{aligned}\right\} \tag{12a}$$

and finally

$$Z_\rho(t) = L^{-1}N_\rho(s) \tag{12b}$$

5. The general case (coupled motion)

In this case it is $z_M \neq 0$ and therefore Eq. (5) are valid. From Eq. (5a), we observe that the vertical motion is independent and therefore the equations of §4.1 are valid. In order for the solution of the problem of coupled lateral-torsional motion to apply the Lagrange's equations, we consider the potential energy of the system.

We call K the kinetic energy, D the dynamic one, F the dissipation energy and Ω the work of the external forces.

5.1 The potential energy of the system

5.1.1 The kinetic energy

The kinetic energy is produced by the lateral-torsional motion of the deck and it is given by the following expression

$$K = \frac{m}{2}\int_0^L \left(\frac{\partial \upsilon}{\partial t}\right)^2 dx + \frac{I_{px}}{2}\int_0^L \left(\frac{\partial \varphi}{\partial t}\right)^2 dx \tag{13a}$$

5.1.2 The dynamic energy

The dynamic energy is caused by the stresses of the deck and the moments produced by the hangers. Thus, from the deck we have

$$\left. D_1 = \frac{1}{2}\int_0^L \left(EI_z\upsilon'''' - EI_z z_M \varphi'''' + B_H \int_0^L \upsilon dx \right)\cdot \upsilon dx + \frac{1}{2}\int_0^L (EI_w\varphi'''' - EI_z z_M \upsilon'''' - GI_d\varphi'')\cdot \varphi dx \right\} \tag{13b}$$

while from the moments of the hangers we get: $m_T = -b^2 B_V \int_0^L \varphi dx + (z_M - \alpha)B_H \int_0^L \upsilon dx$ and

$$D_2 = \frac{1}{2}\int_0^L m_T \varphi dx = \frac{1}{2}\int_0^L \left(-b^2 B_V \int_0^L \varphi dx + (z_M - \alpha)B_H \int_0^L \upsilon dx \right)\cdot \varphi dx \tag{13c}$$

Therefore, the total dynamic energy will be

$$D = D_1 + D_2 \tag{13d}$$

5.1.3 The dissipation energy

The dissipation energy of the system will be

$$F = \frac{1}{2}\int_0^L c_z \dot{\upsilon}^2 dx + \frac{1}{2}\int_0^L c_\varphi \dot{\varphi}^2 dx \tag{13e}$$

5.1.4 The work of the external forces

Finally, the work produced by the external forces is

$$\Omega = \int_0^L (p_y \cdot \upsilon + m_x \cdot \varphi - c_z \dot{\upsilon}_o \upsilon - m\ddot{\upsilon}_o \upsilon)\, dx \tag{13f}$$

5.2 The solution of the equations of the problem

We are searching for a solution of the form

$$\left.\begin{aligned} \upsilon(x,t) &= \sum_n V_n(x) R_n(t) \\ \varphi(x,t) &= \sum_n \Phi_n(x) R_n(t) \end{aligned}\right\} \tag{14}$$

where $R_n(t)$ are the time functions under determination and $V_n(x)$, $\Phi_n(x)$ are functions arbitrarily chosen that satisfy the boundary conditions. As such functions we choose the shape functions given by Eqs. (9b) and (10b), respectively.

5.2.1 The kinetic energy

Introducing Eq. (14) into Eq. (13a), we have

$$K = \frac{m}{2}\int_0^L \left(\sum_n V_n \dot{R}_n\right)^2 dx + \frac{I_{px}}{2}\int_0^L \left(\sum_n \Phi_n \dot{R}_n\right)^2 dx =$$

$$= \frac{m}{2}\int_0^L \sum_n V_n^2 \dot{R}_n^2 dx + \frac{m}{2}\int_0^L \sum_n \sum_k 2 V_n V_k R_n R_k dx + \frac{I_{px}}{2}\int_0^L \sum_n \Phi_n^2 \dot{R}_n^2 dx + \frac{I_{px}}{2}\int_0^L \sum_n \sum_k 2\Phi_n \Phi_k R_n R_k dx$$

From the above equation successively we obtain

$$\frac{\partial K}{\partial \dot{R}_\rho} = m\int_0^L \sum_{k=1}^n V_k V_\rho \dot{R}_k dx + I_{px}\int_0^L \sum_{k=1}^n \Phi_k \Phi_\rho \dot{R}_k dx\,.$$

After differentiation and taking into account the orthogonality conditions of V_ρ and Φ_ρ we obtain

$$\frac{d}{dt}\left(\frac{\partial K}{\partial \dot{R}_\rho}\right) = \ddot{R}_\rho \int_0^L (m V_\rho^2 + I_{px} \Phi_\rho^2)\, dx \tag{15a}$$

In addition

$$\frac{\partial K}{\partial R_\rho} = 0 \tag{15b}$$

5.2.2 The dynamic energy

Introducing (14) into (13d) and taking into account the orthogonality conditions we get

$$D = \frac{1}{2}\int_0^L \left(EI_z \sum_n V_n'''' R_n - EI_z z_M \sum_n \Phi_n'''' R_n + B_H \int_0^L \sum_n V_n R_n dx \right) \cdot \sum_n V_n R_n dx$$

$$+ \frac{1}{2}\int_0^L \left(EI_w \sum_n \Phi_n'''' R_n - EI_z z_M \sum_n V_n'''' R_n - GI_d \sum_n \Phi_n'' R_n \right) \cdot \sum_n \Phi_n R_n dx$$

$$+ \frac{1}{2}\int_0^L \left(-b^2 B_V \int_0^L \sum_n \Phi_n R_n dx + (z_M - \alpha) B_H \int_0^L \sum_n V_n R_n dx \right) \cdot \int_0^L \sum_n \Phi_n R_n dx$$

From the above equation we get

$$\left.\begin{aligned}\frac{\partial D}{\partial R_\rho} &= EI_z R_\rho \int_0^L V_\rho''^2 dx - EI_z z_M \sum_{k=1}^{n}\left\{R_k \int_0^L (\Phi_\rho'' V_k'' + \Phi_k'' V_\rho'')dx\right\} + B_H \int_0^L V_\rho dx \int_0^L \sum_n V_n R_n dx \\ &+ EI_w R_\rho \int_0^L \Phi_\rho''^2 dx + GI_d \int_0^L \left(\Phi_\rho' \sum_n \Phi_n' R_n\right) dx - b^2 B_V \int_0^L \Phi_\rho dx \int_0^L \sum_n \Phi_n' R_n dx \\ &+ \frac{(z_M - \alpha)}{2} B_H \left(\int_0^L V_\rho dx \int_0^L \sum_n \Phi_n R_n dx + \int_0^L \Phi_\rho dx \int_0^L \sum_n V_n R_n dx\right)\end{aligned}\right\} \quad (15c)$$

5.2.3 The dissipation energy

Introducing (14a) into (13e) we obtain

$$F = \frac{1}{2} c_z \int_0^L \left(\sum_n V_n \dot{R}_n\right)^2 dx + \frac{1}{2} c_\varphi \int_0^L \left(\sum_n \Phi_n \dot{R}_n\right)^2 dx$$

which concludes to the following relation

$$\frac{\partial F}{\partial \dot{R}_\rho} = \dot{R}_\rho \left(c_z \int_0^L V_\rho^2 dx + c_\varphi \int_0^L \Phi_\rho^2 dx\right) \quad (15d)$$

5.2.4 The work of the external forces

Introducing (14a) into (13f) we obtain

$$\Omega = \int_0^L p_y(x) f_y(t) \cdot \sum_n V_n R_n dx + \int_0^L m_x(x) f_x(t) \cdot \sum_n \Phi_n R_n dx - \{c_y \dot{\upsilon}_o(t) + m\ddot{\upsilon}_o(t)\} \int_0^L \sum_n V_n R_n dx$$

From the above we obtain

$$\frac{\partial \Omega}{\partial R_\rho} = f_y(t) \int_0^L p_y(x) V_\rho dx + f_x(t) \int_0^L m_x(x) \Phi_\rho dx - \{c_y \dot{\upsilon}_o(t) + m\ddot{\upsilon}_o(t)\} \int_0^L V_\rho dx \quad (15e)$$

5.2.5 The Lagrange's equations

Applying the Lagrange's equations

$$\left.\begin{aligned}&\frac{d}{dt}\left(\frac{\partial K}{\partial \dot{R}_\rho}\right) - \frac{\partial K}{\partial R_\rho} + \frac{\partial D}{\partial R_\rho} + \frac{\partial F}{\partial \dot{R}_\rho} = \frac{\partial \Omega}{\partial R_\rho} \\ &\text{for} \quad \rho = 1 \text{ to } n\end{aligned}\right\} \quad (16a)$$

and taking into account Eqs. (15a) to (15e) we obtain

$$\left.\begin{aligned}
&\ddot{R}_\rho \int_0^L (mV_\rho^2 + I_{px}\Phi_\rho^2)dx + \dot{R}_\rho \int_0^L (c_z V_\rho^2 + c_\varphi \Phi_\rho^2)dx + R_\rho \int_0^L (EI_z V_\rho''^2 + EI_w \Phi_\rho''^2)dx \\
&- EI_z z_M \sum_{k=1}^{n} \left\{ R_k \int_0^L (\Phi_\rho'' V_k'' + \Phi_k'' V_\rho'')dx \right\} + GI_d \int_0^L \Phi_\rho' \sum_n \Phi_n' R_n dx + B_H \int_0^L V_\rho dx \int_0^L \sum_n V_n R_n dx \\
&- b^2 B_V \int_0^L \Phi_\rho dx \int_0^L \sum_n \Phi_n R_n dx + \frac{(z_M - \alpha)}{2} B_H \left(\int_0^L V_\rho dx \int_0^L \sum_n \Phi_n R_n dx + \int_0^L \Phi_\rho dx \int_0^L \sum_n V_n' R_n dx \right) = \\
&= f_y(t) \int_0^L p_y V_\rho dx + f_x(t) \int_0^L m_x \Phi_\rho dx - c_z \dot{\upsilon}_o(t) \int_0^L V_\rho dx - m\ddot{\upsilon}_o(t) \int_0^L V_\rho dx \\
&\text{with}: \quad \rho = 1 \quad \text{to} \quad n
\end{aligned}\right\} \tag{16b}$$

In order to solve the above differential system (16b) we use the Laplace Transformation putting

$$\left.\begin{aligned}
&LR_\rho(t) = G_\rho(s) \\
&Lf_x(t) = u_x(s) \\
&Lf_y(t) = u_y(s) \\
&L\upsilon_o(t) = U_o(s)
\end{aligned}\right\} \tag{17a}$$

From the above and with initial conditions $R_\rho(0) = \dot{R}_\rho(0) = 0$ we obtain

$$\left.\begin{aligned}
&L\dot{R}_\rho(t) = s \cdot G_\rho(s) \\
&L\ddot{R}_\rho(t) = s^2 \cdot G_\rho(s) \\
&L\dot{\upsilon}_o(t) = s \cdot U_o(s) \\
&L\ddot{\upsilon}_o(t) = s^2 \cdot U_o(s)
\end{aligned}\right\} \tag{17b}$$

Therefore, the system (16b) becomes

$$\left.\begin{aligned}
&A_{\rho 1}G_1 + A_{\rho 2}G_2 + \dots\dots\dots + A_{\rho\rho}G_\rho + .\rho\dots\dots\dots + A_{\rho n}G_n = \Xi_\rho \\
&\text{with} \quad \rho = 1 \quad \text{to} \quad n \quad \text{and}: \\
&A_{\rho k} = -EI_z z_M \int_0^L (\Phi_\rho'' V_k'' + \Phi_k'' V_\rho'')dx + GI_d \int_0^L \Phi_\rho' \Phi_k' dx + B_H \int_0^L V_\rho dx \int_0^L V_k dx \\
&\qquad - b^2 B_V \int_0^L \Phi_\rho dx \int_0^L \Phi_k dx + \frac{(z_M - \alpha)}{2} B_H \left(\int_0^L V_\rho dx \int_0^L \Phi_k dx + \int_0^L \Phi_\rho dx \int_0^L V_k dx \right) \\
&A_{\rho\rho} = s^2 \cdot \int_0^L (mV_\rho^2 + I_{px}\Phi_\rho^2)dx + s \cdot \int_0^L (c_z V_\rho^2 + c_\varphi \Phi_\rho^2)dx + \int_0^L (EI_z V_\rho''^2 + EI_w \Phi_\rho''^2)dx \\
&\qquad - 2EI_z z_M \int_0^L \Phi_\rho'' V_\rho'' dx \\
&\qquad + GI_d \int_0^L \Phi_\rho'^2 dx + B_H \left(\int_0^L V_\rho dx \right)^2 - b^2 B_V \left(\int_0^L \Phi_\rho dx \right)^2 + (z_M - \alpha) B_H \int_0^L V_\rho dx \int_0^L \Phi_\rho dx \\
&\Xi_\rho = u_y(s) \int_0^L p_y V_\rho dx + u_x(s) \int_0^L m_x \Phi_\rho dx - c_y s U_o(s) \int_0^L V_\rho dx - ms^2 U_o(s) \int_0^L V_\rho dx
\end{aligned}\right\} \tag{17c}$$

Solving the above system we get the functions $G_\rho(s)$ and therefore

$$R_\rho(t) = L^{-1} G_\rho(s) \tag{17d}$$

6. Numerical results and discussion

In this section, a numerical investigation based on the equations obtained in the previous paragraphs has been developed. The main goal of the presented examples is to search the influence of an inclined cables system mainly on the lateral motion of the bridge and also the effect of this inclination on the bridge's capacity to suffer vertical and torsional motion.

Lets us consider therefore a suspension bridge like the one of Fig. 3, with the following characteristics: $L_1 = L_3 = 200\,\mathrm{m}$, $L_2 = 1000\,\mathrm{m}$, $h = f_o = 120, 100, \text{and } 80\,\mathrm{m}$, $b = 12.50\,\mathrm{m}$.

The cross-section's data is: Cross-sectional area: $F = 0.700\mathrm{m}^2$, and resistance moments: $I_y = 0.125\,\mathrm{m}^4$, $I_z = 10.600\,\mathrm{m}^4$, $I_d = 1.15\cdot10^{-5}\,\mathrm{m}^4$, $I_\omega = 4.301\mathrm{m}^6$, $I_{px} = 8.580\,\mathrm{tn}\cdot\mathrm{sec}^2$.

Without restriction of the generality we consider that the cross-section is an of double symmetry one i.e., $z_M = 0$.

The bridge is made from isotropic and homogeneous material with modulus of elasticity $E_b = 2.10\cdot10^6\,\mathrm{dN/cm^2}$ and shear modulus $G = 0.80\cdot10^6\,\mathrm{dN/cm^2}$.

Each of the two suspended cables has area of cross-section $F_c = 0.125\mathrm{m}^2$ and modulus of elasticity $E_c = 2.00\cdot10^6\,\mathrm{dN/cm^2}$, while their limit strength is $\sigma = 8\,000\mathrm{dN/cm^2}$.

The dead load is $g = 0.700\cdot7850 = 5500\,\mathrm{dN/m}$.

Applying the Eqs. (1a) for each cable we can determine:
for $h = 120\,\mathrm{m}$ we get $f'' = -0.00096$ and cable force $H_o = 2\,850\,000\,\mathrm{dN/cable}$
for $h = 100\,\mathrm{m}$ we get $f'' = -0.00081$ and cable force $H_o = 3\,437\,000\,\mathrm{dN/cable}$
for $h = 80\,\mathrm{m}$ we get $f'' = -0.00064$ and cable force $H_o = 4\,297\,000\,\mathrm{dN/cable}$

The cable-system, may be inclined to the outward or to the inward of the bridge (see Fig.3c). For the first case there is not a geometrical restriction, but for the second one the angle of inclination must satisfy the inequality: $\sin\theta \le b/h$.

For a constant width of the deck $2b = 25\,\mathrm{m}$, we have

$$\left.\begin{array}{lll} \text{For} & h = 120\,\mathrm{m}: & \theta \le 6^o \\ \text{For} & h = 100\,\mathrm{m}: & \theta \le 7.10^o \\ \text{For} & h = \ 80\,\mathrm{m}: & \theta \le 9^o \end{array}\right\}$$

6.1 The lateral motion

In order to study the lateral motion and the influence of the inclined cable-system, we consider a distant source earthquake given by the equation $\upsilon_o(t) = \alpha\cdot t\cdot e^{-k\cdot t}\sin\Omega t$, (with $\alpha = 0.05$, $k = 0.5$, and $\Omega = 12$). Therefore, we get the following diagrams of Fig. 7, showing the soil motion and its acceleration.

6.1.1 The influence of angle θ

Applying the equations of §4.2 for $f_o = 120\,\mathrm{m}$ and $\theta = 0^o$, 2^o, 4^o, and 6^o, we obtain the plots

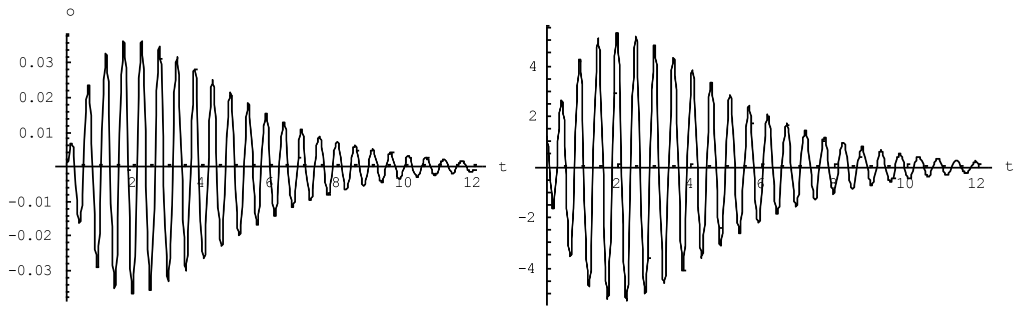

Fig. 7 Soil motion (m) and acceleration (m/s^2) with respect to time t (s) caused by a distant earthquake

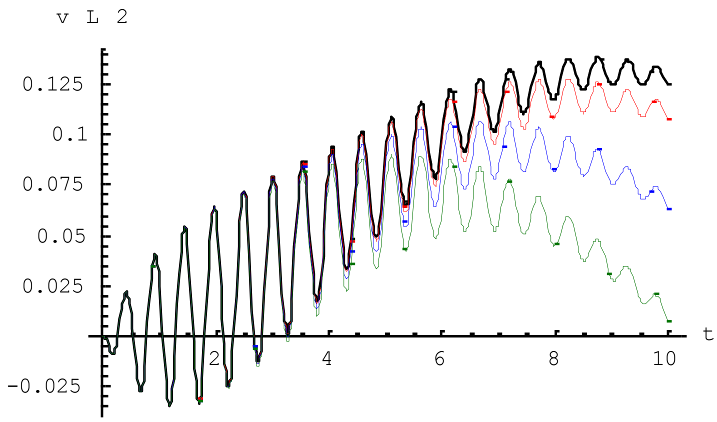

Fig. 8 The influence of angle θ on the lateral deflections (m) of the middle of the bridge for θ=0º(black), θ=2º(red), θ=4º (blue) and θ=6º (green)

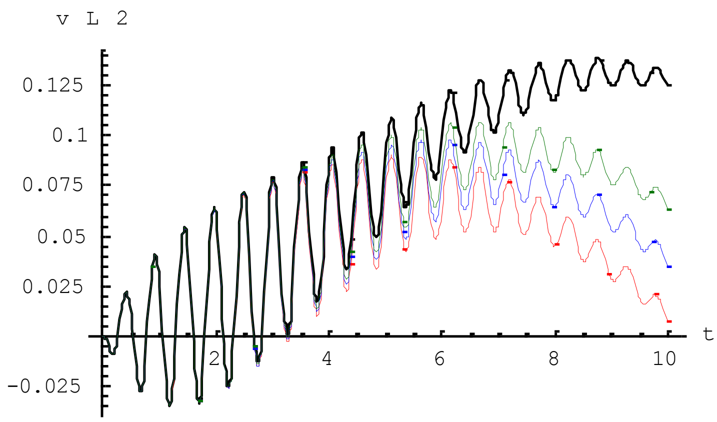

Fig. 9 The influence of sag f_o on the lateral deflections (m) of the middle of the bridge for f_o=120 m and θ=0º(black), f_o=120 m and θ=6º (red), f_o=100 m and θ=6º (blue) and, f_o=80 m and θ=6º θ=6º (green)

of Fig. 8 giving the motion of the middle of the bridge.

We ascertain that even for small values of angle θ its influence on the lateral motion is notable.

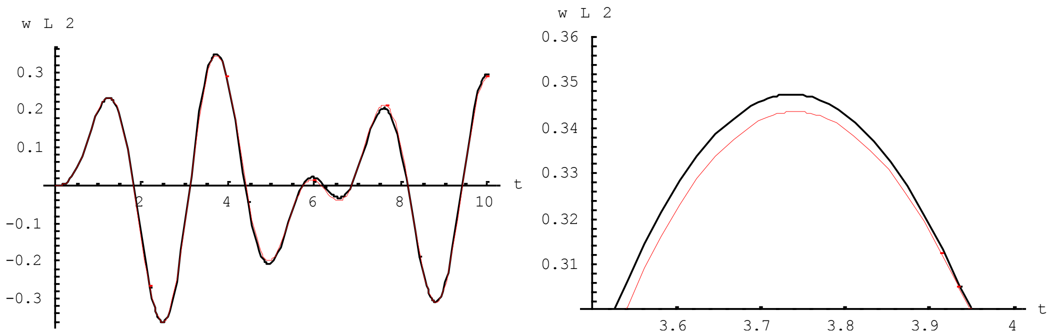

(a) (b)

Fig. 10 The vertical motion (m) of the middle of the bridge (black) bridge with $\theta=0^{O}$ and (red) bridge with $\theta=6^{O}$

Particularly for $\theta = 2^{\circ}$ the decrease of the deformation amounts to 10.7%, for $\theta = 4^{\circ}$, to 25% while for $\theta = 6^{\circ}$ to 39.2%.

6.1.2 The influence of sag f_o

The size of the sag f_o affects the influence of the angle of inclination θ. In the following plots of Fig. 9 we see the influence of a constant angle $\theta = 6^{\circ}$ on the lateral motion in relation with the size of sag f_o.

Particularly, for a constant angle $\theta = 6^{\circ}$ the decrease of the deformation amounts to 38.90% for $f_o = 120\,\mathrm{m}$, to 32.00% for $f_o = 100\,\mathrm{m}$, and to 25.10% for $f_o = 80\,\mathrm{m}$.

6.2 The vertical motion

It is obvious that the ability of the bridge to undertake vertical loads is affected by the inclination of the cable-system.

In order to estimate this change of ability we consider a cable system inclined by $\theta=6^{o}$ and sag f_o=120m. In addition, we apply the dynamic load $p(t) = 500 \cdot \sin 3t\ \mathrm{dN/m}$, extended from $x = L_2/4$ to $x = 3L_2/4$.

Applying the equations of §4.1 we obtain the plots of Fig. 10(a), where is shown the vertical motion of the middle of the bridge for $\theta = 0^{\circ}$ and sag $f_o = 120\,\mathrm{m}$ (black) and $\theta = 6^{\circ}$ and sag $f_o = 120\,\mathrm{m}$ (red). Fig. 10(b) is a blow-up of the plot 10a for $t = 3.5$ to $4\,\mathrm{sec}$.

From this last plot we ascertain that there is a slight change (increase) in the bridge ability, which is about 0.71%.

6.3 The torsional motion

In order to study the bridge's behavior in torsional motion, we consider that the above in §6.2

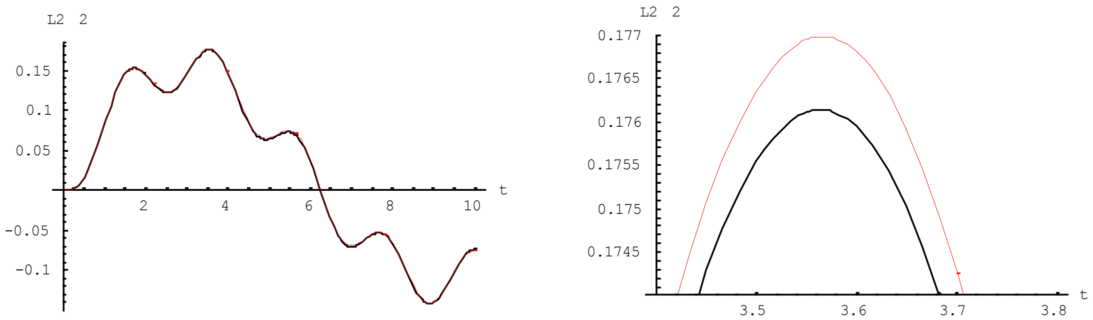

(a) (b)

Fig. 11 The torsional motion (rad) of the middle of the bridge (black) bridge with θ=0^{O} and (red) bridge with θ=6^{O}

dynamic loading acts eccentric in a distance $e_k = 5.0\,\mathrm{m}$ from the axis of the cross-section.

Applying the equations of §4.3 we obtain the plots of Fig. 11(a), where is shown the torsional motion of the middle of the bridge for $\theta = 0°$ and sag $f_o = 120\,\mathrm{m}$ (black) and $\theta = 6°$ and sag $f_o = 120\,\mathrm{m}$ (red). Fig. 11(b) is a blow-up of the plot 11a for $t = 3.4$ to $3.8\,\mathrm{sec}$.

From this last plot we ascertain that there is a slight change (decrease) in the bridge ability, which is about 0.52%.

7. Conclusions

From the above bridge model and the results presented herein, one can draw the following conclusions:

• A mathematical model for the study of suspension bridges with inclined cable-system and their dynamic behavior is proposed.

• Even for small values of angle θ of the inclined cable-system one can see a significant influence on the lateral motion which ranges from 10.7% ($\theta = 2°$) to 39.2% ($\theta = 6°$). If the system is inclined inwards the bridge, the value of the angle θ has a limit value depending on the ratio b/h of the half cross-section width to the height of the pylon. Contrarily, for an outward inclination of the cable-system, there is no such a limit (except the one which depends on the pylon's strength) and therefore, the influence of the inclined system on the lateral deformation increases.

• The height h of the pylon (for the same angle θ), strongly affects the influence of the inclined cable-system on the lateral motion. This effect ranges from 25% to 40%.

• The inclination of the cable-system does not affect significantly the bridge regarding its ability to undertake vertical or torsional loadings. This influence is very weak and ranges in rates less than 0.8%.

• Finally, one can ascertain that a detailed design should take into account all combinations of the above factors involved in the preceding analysis.

References

Am. Association of State (1977), *Standard Specifications for Highway Bridges*, 12th Edition, Hwy and Transp. Officials (AASHTO), Washington, U.S.A.

Baloevic, G., Radnic, J., Ggric, N., Matesan, D. and Smilovic, M. (2016), "Numerical model for nonlinear analysis of composite concrete-steel-masonry bridges", *Coupled Syst. Mech.*, **5**(1), 1-20

Cantieri, R. (1991), *Beitrag zur Dynamik von Strassenbrucken Unter der Uberfahrt Schwerer Fahrzeuge*, Diss. ETH Nr 9505, Technische hochschule, Zurich.

Council of Eur. Communities (1992), *Council Directive, 92/7/EEC Amending Directive 85/3/EEC on the Weights, Dimensions and Certain Technical Characteristics of Certain Road Vehicles*, Brussels, Belgium.

Eckhard, B. and Ott, E. (2006), "Crowd synchrony on the London millennium bridge", *Chaos*, **16**(4), 041104.

Foda, M.A. and Abduljabbar, Z. (1972), "A dynamic green function formulation for the response of a beam structure to a moving mass", *J. Sound Vibr.*, **210**(3).

Frýba, L. (1972), *Vibrations of Solids and Structures under Moving Loads*, Groningen, Nordhoff International Publication Co.

Gillespi, T.D. (1993), *Effect of Heavy Vehicle Characteristics on Pavement Response and Performance*, NCHRP, Rep. 353, Trans Res. Board (TRB), Washington, U.S.A.

Greco, F., Lonetti, P. and Pascuzzo, A. (2013), "Dynamic analysis of cable-stayed bridges affected by accidental failure mechanisms under moving loads", *Math. Prob. Eng.*

Green, M.F. and Cebon, D. (1994), "Dynamic response of highway bridges to heavy vehicle loads: Theory and experimental validations", *J. Sound Vibr.*, **170**(1).

Green, M.F., Cebon, D. and Cole, D.J. (1995), "Effects of vehicle suspension design on dynamics of highway bridges", *J. Struct. Eng.*, **121**(2).

Hillerborg, A. (1951), *Dynamic Influences of Smoothly Running Loads of Simply Supported Girders*, Kungl. Tekhn. Högs kolan, Stockholm.

Honda, H., Kajikawa, Y. and Kobori, T. (1982), "Spectra of road surface roughness on bridges", *J. Struct. Eng.*, **108**(9).

Inglis, C.E. (1934), *A Mathematical Treatise on Vibration in Railway Bridges*, Cambridge University Press, Cambridge.

Ingolfsson, E.T. and Georgakis, C.T. (2001), "A stochastic load model for pedestrian-induced lateral forces on footbridges", *Eng. Struct.*, **33**(12), 3454-3470.

Ingolfsson, E.T., Georgakis, C.T. and Jonsson, J. (2012), "Pedestrian-induced lateral vibrations of footbridges: A literature review", *Eng. Struct.*, **45**, 21-52.

ISO/TC 108/WG9 Draft No 3c, Int. Organization for Standarization (ISO), Geneva, Switzerland (1972), *Proposals for Generalized Road Inputs to Vehicles*.

Jeffcott, H.H. (1929), "On the vibration of beams under the action of moving loads", *Philosoph. Mag., Ser.*, **7-8**(48), 66-67.

Krýlov, A.N. (1905), *Mathematical Collection of Papers of the Academy of Sciences*, St. Petersburg, **61**.

Krýlov, A.N. (1905), "Über die erzwungenen schwingungen von gleichförmigen elastigchen stäben", *Math. Annal.*, **61**, 211.

Lee, H.P. (1996), "Dynamic response of a beam with a moving mass", *J. Sound Vibr.*, **191**(2).

Li, Z., Li, P., He, Z. and Cao, P. (2013), "Static and free vibration analysis of shallow sagging inclined cables", *Struct. Eng. Mech.*, **45**(2), 145-157.

Lonetti, P. and Pascuzzo, A. (2014), "Design analysis of the optimum configuration of self-anchored cable-stayed suspension bridges", *Struct. Eng. Mech.*, **51**(5), 847-866.

Lonetti, P. and Pascuzzo, A. (2014), "Vulnerability and failure analysis of hybrid cable-stayed suspension bridges subjected to damage mechanisms", *Eng. Fail. Analy.*, **45**, 470-495.

Michaltsos, G.T. (2001), "The influence of centripetal and coriolis forces on the dynamic response of light bridges under moving vehicles", *J. Sound Vibr.*, **247**(2), 261-277.

Michaltsos, G.T. (2002), "Dynamic behaviour of a single-span beam subjected to load moving with variable speeds", *J. Sound Vibr.*, **258**(2), 359-372.

Michaltsos, G.T., Sophianopoulos, D. and Kounadis, A.N. (1996), "The effect of a moving mass and other

parameters on the dynamic response of a simply supported beam", *J. Sound Vibr.*, **191**(3), 357-362.
Ministry of Transport and Communications (1983), *Ontario Highway Bridge Design Code*, Ontario, Canada.
Nakamura, S. and Kawasaki, T. (2006), "Lateral vibration of footbridges by synchronous walking", *J. Constr. Steel Res.*, **62**(11), 1148-1160.
Raftoyiannis, I.G., Konstantakopoulos, T.G. and Michaltsos, G.T. (2014), "Dynamic response of cable-stayed bridges subjected to sudden failure of cables-the 2D problem", *Coupled Syst. Mech.*, **3**(4), 345-365.
Roberts, G.W., Mengbrown, C.J. and Dallard, P. (2008), "GPS measurements on the London millennium bridge", *Proceedings of the Institution of Civil Engineers: Bridge Engineering*, **159**(4), 153-161.
Saller, H. (1921), *Einfluss Bewegter Last Auf Eisenbahnoberbau Und Brücken*, Kreidels Verlag, Berlin, Germany.
Steuding, H. (1934), "Die schwingungen von trägern bei bewegten lasten I, II", *Ingen. Archiv.*, **5**(4), 275-305/1935, **6**(4), 265-270.
Stokes, G.G. (1849), *Discussion of a Differential Equation Relating to the Breaking of Railway Bridges*, Transactions of the Cambridge Philosophical Society, 707-735.
Sun, B., Zhang, L., Qin, Y. and Xiao, R. (2016), "Economic performance of cable supported bridges", *Struct. Eng. Mech.*, **59**(4), 621-652.
Timoshenko, S.P. (1922), "On the forced vibration of bridges", *Philosoph. Mag.*, **43**, 1018.
Xu, X., Xu, W. and Genin, J. (1997), "A non-linear moving mass problem", *J. Sound Vibr.*, **204**(3).
Zhang, X. and Yu, Z. (2015), "Study of seismic performance of cable-stayed-suspension hybrid bridges", *Struct. Eng. Mech.*, **55**(6), 1203-1221.
Zhang, X. and Zhang, C. (2016), "Study of seismic performance and structural system of suspension bridges", *Struct. Eng. Mech.*, **60**(4), 595-614.
Zibdeh, H.S. and Reckwitz, R. (1996), "Moving loads on beams with general boundary conditions", *J. Sound Vibr.*, **195**(1).
Zimmermann, H. (1896), *Die Schwingungen Eines Trägers Mit Bewegter Last*, Centralblatt der Bauverwaltung, **16**(23), 249-251, **23**A, 257-260, **24**, 264-266, **26**, 288.

CC

Nomenclature

υ	horizontal displacement
w	vertical displacement
φ	rotation
h, h_o	pylon heights
f_o	cable sag
N	tension force
H,V	force components (horizontal and vertical)
S	hanger forces

$(\ )_o$	components due to dead loads
$(\ )_e$	components due to live or dynamic loads
$(\ )_H$	horizontal components
$(\ )_V$	vertical components
EI	bending stiffness
c	damping
m	mass per unit length
K	kinetic energy
D	dynamic energy
F	dissipation energy
ω	frequency
T,R,Z	time functions
W,V,Φ	shape functions